



We are Nitinol.™

## **Hydrogen Effects on Nitinol Fatigue**

J. Sheriff, A. R. Pelton and L.A. Pruitt,

Proceedings of ASM Materials & Processes for Medical Devices Conference, eds: M. Helmus and D. Medlin, 38-43 (2005).

2005

## Hydrogen Effects on Nitinol Fatigue

J. Sheriff, A.R. Pelton

Nitinol Devices and Components, Fremont, CA, USA

L.A. Pruitt

Department of Bioengineering and Mechanical Engineering, University of California, Berkeley, CA, USA

### Abstract

This paper summarizes recent investigations of the influence of hydrogen on superelastic Nitinol (NiTi) and its effect on fatigue properties. NiTi is used in applications such as arterial stents, vena cava filters, and endodontic files where fatigue performance is a critical design component. ASTM Standard F-2063-00 limits hydrogen concentration to 50wppm for wrought NiTi products (bar, wire, tube) used in the manufacture of medical devices and other surgical instruments. To date, however, no studies have linked this hydrogen standard to fatigue performance. The data presented here suggest hydrogen concentrations as low as 50wppm cause a small yet statistically significant decrease in fatigue life above 1.4% strain. Increasing hydrogen concentration does not appear to affect fatigue life at or below 1.4% strain up to 80wppm hydrogen. The data presented here also show a second low cycle fatigue regime previously not analyzed with Coffin-Manson approximations for transforming NiTi.

### Introduction

Nitinol (NiTi) has many commercial applications including cell phone antennae wire, eyeglass frames, and orthodontic wire, that take advantage of the unique engineering properties of the material. NiTi is also increasingly used in medical applications where fatigue performance is critical, such as in arterial stents, vena cava filters, and endodontic files [1]. Pelton, *et al.* point out that finished Nitinol products are typically processed in hydrogen containing environments, including electropolishing, electroplating, and soldering [2]. It is clear from previous research that the mechanical properties of Nitinol in hydrogen containing environments differ from those in the absence of hydrogen [2-11]. It therefore follows that the effect of hydrogen must be considered when designing processing techniques and commercial applications for NiTi. Fatigue properties of hydrogen-containing NiTi medical devices are of particular interest because previous studies suggest that NiTi can absorb hydrogen from the body [7].

There has been steady refinement in the published literature about the microstructural nature of hydrogen in NiTi. The concentration at which NiTi forms a hydride instead of remaining in a solid solution is a topic of ongoing discussion. Pelton, *et al.* used x-ray diffraction studies and observed a tetragonal hydride phase at concentrations as low as 75 wppm hydrogen [8-9]. Several investigations have shown the presence of NiTi-hydrides under various conditions of

temperature and pressure [10-13]. Asaoko, *et al.* investigated the effect of hydrogen on the mechanical and shape memory properties of NiTi and showed that small amounts of hydrogen (10-50wppm) affected the cyclic shape memory properties as well as the mechanical properties of NiTi [3]. They proposed that their concentration was insufficient to form hydrides; rather that interstitial hydrogen interacted with dislocations. They further proposed that brittle behavior resulted from hydrogen trapped at martensite grain boundaries, twin interfaces, or dislocations.

Three recent studies clearly show that hydrogen tends to form concentration gradients near the sample surfaces in hydrogenated NiTi. These gradients are observed by SEM [2,4] and hardness measurements [4]. Furthermore, high residual hydrogen concentrations were measured on wires with 800wppm that were sequentially centerless ground and analyzed [8-9].

Fatigue behavior has also been studied extensively on both shape memory and superelastic NiTi [14-19]. Surprisingly, however, there is a dearth of published literature on the effects of hydrogen effects on fatigue behavior. ASTM F-2063-00 specifies a limit of 50wppm hydrogen for wrought NiTi products (bar, wire, tube) used in the manufacture of medical devices [20]. The reports of hydride formation with as low as 75 wppm H in austenitic and martensitic NiTi provides motivation to explore the fatigue properties of NiTi with up to 100 wppm hydrogen. This paper therefore summarizes an investigation performed to better understand the influence of hydrogen on superelastic NiTi and its effect on the fatigue properties of Nitinol.

### Materials and Methods

Electropolished NiTi wire with an  $A_f$  temperature of 13°C and 0.8mm diameter with nominal 10 wppm H was hydrogenated at 80°C in 85% phosphoric acid for various times. Target hydrogen concentrations were 35, 50, and 80wppm. Multiple samples from each condition were analyzed by vacuum fusion hydrogen analysis at Luvak, Inc. (Boylston, MA).

Up to five samples each were fatigue tested at approximately 4.3%, 3.4%, 2.8%, and 2.0% half-amplitude alternating strain using custom built rotary bending equipment [21]. Up to 15 samples each were tested at 1.4%, 0.7%, and 0.5% half amplitude alternating strain. Strain was estimated with  $\epsilon = r / \rho$  where  $\epsilon$  is strain,  $r$  is the wire radius, and  $\rho$  is the radius of

curvature [22]. Each test was run in a room temperature (19-23°C) water bath to a maximum of  $10^7$  cycles. The fracture surfaces were inspected after fatigue testing with a JEOL JSM 5600 SEM in secondary electron image (SEI) mode at 20KeV from 100 to 1000X. Of particular interest in these microstructural studies was the comparison of the fracture initiation and overall nature of deformation.

### Results and Discussion

Figure 1 shows half-amplitude strain versus cycles to failure ( $\epsilon/N$ ) data for the 10wppm hydrogen wires. Note that multiple wires tested at 0.55% alternating strain were terminated without fracture at  $10^7$  cycles. The endurance limit, or the lowest value of strain that caused failure, was determined to be 0.7%. Overall, these 10wppm hydrogen fatigue data compare favorably to previous published rotary bend fatigue data, although no previous study explored the highest strain levels presented here [16-17].

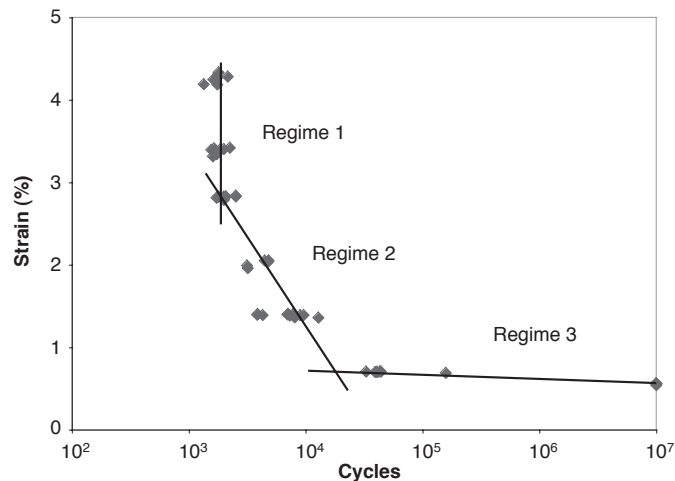


Figure 1: Raw  $\epsilon/N$  data from as-electropolished wires. Note the three distinct strain regions and the 0.7% endurance limit.

Three trend lines can be fit to these data which correspond to three distinct regimes of the  $\epsilon/N$  curve labeled in Figure 1. Regime 1 ( $\leq 10^3$  cycles) extends from 4.5% to approximately 2.75% strain; Regime 2 represents strains from 2.75% to 0.75%. Regime 3 corresponds to high-cycle fatigue ( $>10^4$  cycles).

Figure 2 shows half-amplitude strain versus cycles to failure ( $\epsilon/N$ ) data for all wires tested during this study along with the trend lines from Figure 1. It appears that the higher hydrogenated samples follow the same general trends as the electropolished wires. Furthermore, wires with each hydrogen concentration also reached  $10^7$  cycles at low strain levels without failure. Three important and general observations can be observed from these data, independent of hydrogen content:

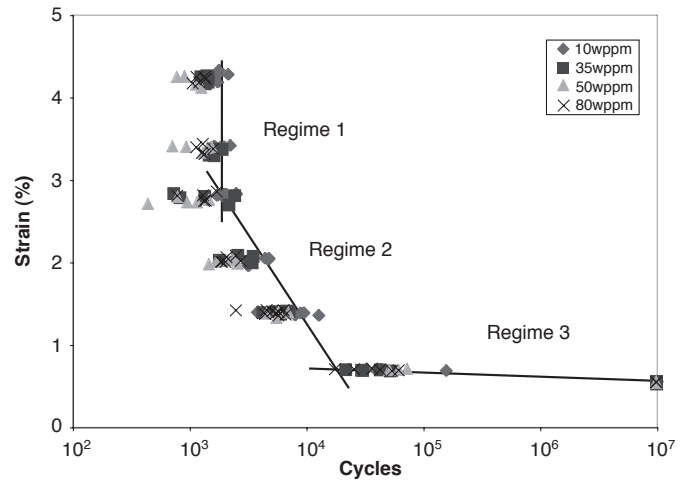


Figure 2:  $\epsilon/N$  data 10, 35, 50, and 80wppm H samples show similar trends with decreasing fatigue life with increasing hydrogen.

1. The low-cycle fatigue data (Regime 1) are nearly independent of strain and the life data are on the order of  $10^3$  cycles.
2. Decreasing strain in the intermediate strain range (Regime 2) leads to increasing fatigue life in the range of  $10^3$  to  $10^5$  cycles.
3. Higher cycle fatigue (Regime 3) is observed at the lower strains with larger deviations in the average cycle life.

Furthermore, although the effects are not large, the hydrogenated samples tend to decrease average fatigue life at alternating strains above approximately 1.4%. Note that the hydrogenated samples tend to fall to the low-cycle side of the 10-wppm hydrogen trend lines in Regimes 1 and 2. However, no clear trend is evident at or below 1.4%. In order to determine if this low-cycle fatigue behavior is statistically significant, analysis of variance (ANOVA) was calculated with Minitab™ Statistical Software version 13.32. Table I summarizes average (AVG) and standard deviation (STDEV) fatigue life (N) data for strain levels at and above 1.4%.

Table I: Average and Standard Deviation Fatigue Life Data

Strain Level	10 wppm		35 wppm		50 wppm		80 wppm	
	AVG	STDEV	AVG	STDEV	AVG	STDEV	AVG	STDEV
4.25%	1739	241	1394	79	1013	198	1249	135
3.40%	1789	233	1645	166	1206	356	1353	169
2.75%	2082	297	1520	780	981	394	1326	338
2.00%	4080	844	2960	734	2083	470	2222	363
1.40%	7323	2686	6717	1069	5655	883	5596	1272

ANOVA ( $\beta = 0.10$ ) shows statistically significant differences between 10wppm samples and those at 50 and 80wppm hydrogen in Regime 1 ( $p < 0.001$  at 4.25% strain,  $p = 0.002$  at 3.4% strain and  $p = 0.004$  at 2.75% strain). At 4.25% strain 10wppm samples are also statistically different from 35wppm samples ( $p < 0.001$ ). At 3.4% and 2.75% strain 35wppm

samples are not significantly different from 10wppm samples;  $p = 0.001$  and  $0.004$ , respectively.

The fatigue life at 2.0% strain and with 35wppm was not different from the 10wppm behavior ( $p < 0.001$ ). However, the 50 and 80wppm fatigue life were statistically lower ( $p < 0.001$ ). At lower strains there is considerably more overlap in the data compared to Regime 1 and it follows that no hydrogen concentration level is statistically different from another ( $p = .119$  at 1.4% strain).

In Regime 3 the life-cycle data are not normal and therefore cannot be analyzed using ANOVA. However, it is clear that increasing hydrogen content within this limited range does not consistently decrease fatigue life.

Figures 3-5 illustrate representative SEM images from Regime 1, Regime 2, and Regime 3, respectively, for each hydrogen level. All samples showed crack initiation on the outer surface of the wire, subsequent crack propagation, and then final failure. Furthermore, typical of other SEM studies of NiTi fatigue, no characteristic fatigue striations were observed [19]. In addition, no systematic differences in the fracture initiation sites from each of the three regimes or with hydrogen content.

Despite the number of investigations of the NiTi-H system, there have been no comprehensive studies on the mechanisms of hydride formation in NiTi. Insight may be gained, however, by drawing a parallel with studies of hydrogen in titanium-based alloys [23].

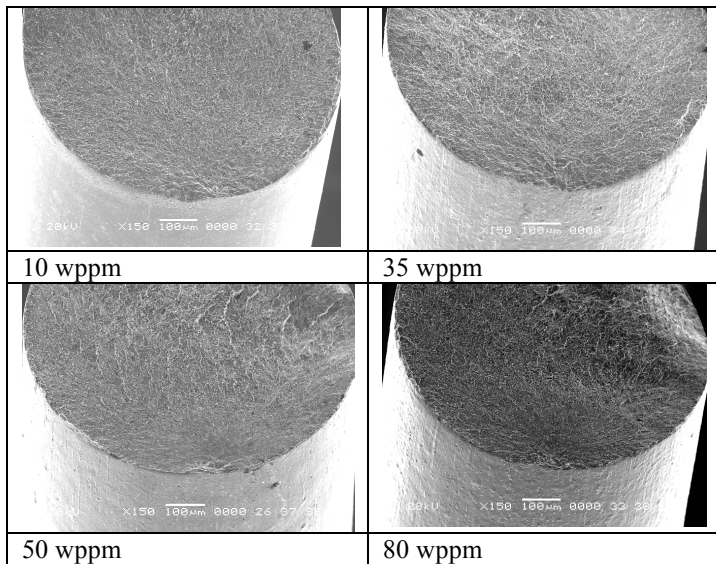


Figure 3: Representative SEM images from all four hydrogen levels at 3.4% strain (Regime 1). All images were taken in SEI mode, 20keV and 150X magnification.

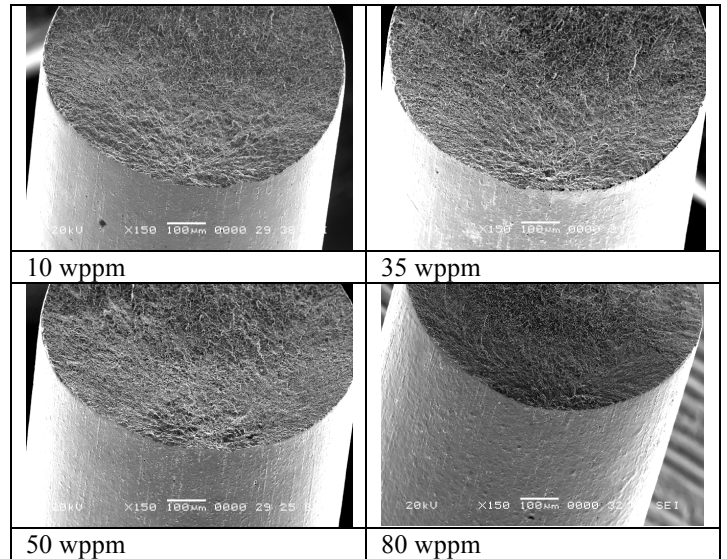


Figure 4: Representative SEM images from all four hydrogen levels at 1.4% strain (Regime 2). All images were taken in SEI mode, 20keV and 150X magnification.

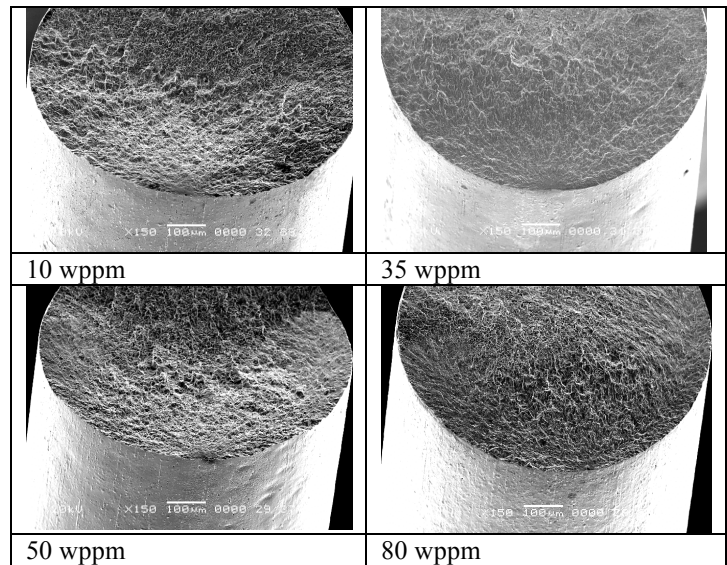


Figure 5: Representative SEM images from all four hydrogen levels at 0.75% strain (Regime 3). All images were taken in SEI mode, 20keV and 150X magnification.

The small size and high mobility of hydrogen atoms promotes easy penetration in Ti alloys pending the breakdown of the titanium oxide ( $\text{TiO}_2$ ) layer via elevated temperature or stress. Once absorbed, hydrogen ions are able to diffuse quickly through the lattice via interstitial sites, dislocations, and grain boundaries. Hydrogen collects in regions of high triaxial stress within solid solution or in hydride phases (commonly  $\text{TiH}_2$  with a  $\text{CaF}_2$  structure and  $4.454 \text{ \AA}$  lattice parameter). Hydrogen transport occurs faster in  $\beta$ -Ti than in  $\alpha$ -Ti due to

the more open bcc ( $\beta$ -Ti) structure. Solid solution hydrogen in either phase causes local lattice expansion and the development of a local strain field.  $\beta$ -Ti can experience up to a 5.35 volume percentage increase due to solid solution hydrogen atoms. Transformation from  $\alpha$ -Ti to the hydride phase causes a 17.2% volume expansion. Because of the significant volume increase, hydride phases tend to form at phase boundaries ( $\alpha/\beta$ ) or other free surfaces where there are less constraint effects than in transgranular hydrides. Once formed, hydrides restrict slip behavior that concentrates stresses and are more brittle than the surrounding matrix, which causes rupture at lower strains [23].

Wu *et al.* [24-25] observed extra "1/2" diffraction reflections in NiTi-H by transmission electron microscopy and proposed that they were due to hydrogen ordering on octahedral sites associated with the Ti sublattice. Analysis of their diffraction data suggests a superlattice with hydrogen occupying only O<sub>y</sub> and O<sub>z</sub> sites that produces a 4 x 2 x 2 tetragonal structure with  $a = 3.0\text{\AA}$  and  $b = c = 3.1\text{\AA}$ . In comparison, equiatomic TiCo [26] and TiFe [27] form hydrides by hydrogen occupying octahedral sites on the B2 lattice; the TiCo hydride has a tetragonal structure with  $a = b = 6.14\text{\AA}$  and  $c = 9.06\text{\AA}$  [26]. Similarly, in the NiTi-H system, Pelton, *et al.* presented x-ray diffraction data with hydride formation as low as 75wppm consistent with a tetragonal unit cell ( $a = b = 6.36\text{\AA}$  and  $c = 9.32\text{\AA}$ ) [9]. Hydrogen was also shown to shift the {110} B2 diffraction peak prior to observation of extra diffraction peaks. These peak shifts to lower angles correspond to an increase in cell volume [8]. Therefore, similar to the Ti-H systems, hydrogen and hydrides cause lattice strain in NiTi.

For rotary-bend fatigue testing, maximum tensile and compressive strain occurs in the wire outer fibers. During each test a single point on the wire surface rotates from maximum tension to maximum compression with a zero mean strain. There is also a radial strain gradient with this mode of deformation with zero strain at the neutral fiber.

In the present investigation, hydrogen decreases average fatigue life above 1.40% strain with an even more pronounced effect above 2.75% strain. These strains roughly correspond to the transition from elastic deformation of austenite and stress-induced martensite for superelastic wire in pure bending conditions; for which there is an increasing volume fraction of martensite with increasing strain. Miyazaki, *et al.* [16] proposed that the deformation modes influence the fatigue behavior of superelastic NiTi during rotary bend testing. To illustrate these effects, the bending behavior of superelastic wire (4°C A<sub>f</sub> tested at 22°C) [28] is shown in Figure 6 with the three regimes marked. As such, three distinct regions that influence the interactions between hydrogen and deformation mechanisms are proposed.

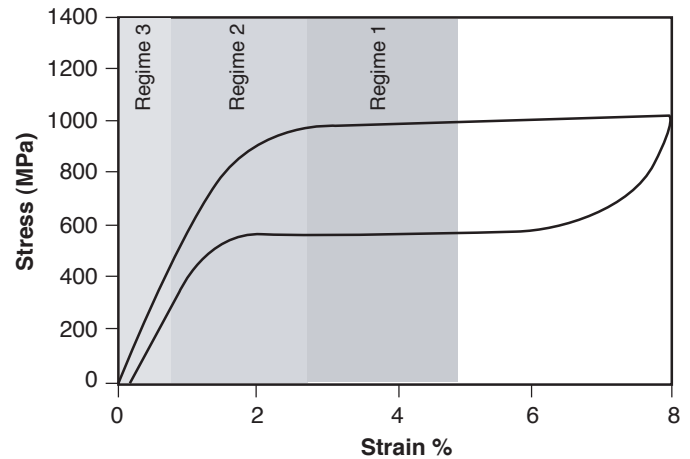


Figure 6: Regime transitions compare favorably to pure bending stress strain data from Wick [28].

The SEM images in Figures 3-5 do not offer strong support for brittle fatigue fracture due to hydride formation as shown with monotonic fracture with larger hydrogen contents [2,4]. Nevertheless, the trend for decreased fatigue life in Regime 1 may result from the effects of interstitial hydrogen or tetragonal hydrides. If hydrogen is concentrated near the outer edge, the high hydrogen regions will superimpose with the high strain regions, thereby reducing the fatigue life. It is also important to recognize that the strains in Regime I correspond to the forward and reverse formation of stress-induced martensite. For example at  $\pm 4\%$  cyclic strain, there is approximately 50% volume formation of stress-induced martensite with 50% strained austenite. It is unclear from the literature if there are any major differences in behavior of hydrogen in stress-induced martensite or strained austenite. It is also interesting to consider the possible effects of hydrogen on the interface between austenite and martensite. However, it has been shown that excessive amounts of hydrogen can decrease the thermal martensitic start transformation, which stabilizes austenite [2]. Yokoyama, *et al.* [10] suggest that hydrogen may be more mobile in stress-induced martensite than in austenite, thus increasing the potential for high surface hydrogen to coincide with the stress-induced martensite regions. These investigators observed that hydrogen embrittled NiTi fractures more quickly when held at stresses above the critical martensite transformation stress compared to stresses below the critical martensite transformation stress. The authors also observed higher hydrogen absorption in the mixed stress-induced martensite and strained austenite than in stress-free austenite. As discussed earlier for Ti-based alloys, it is expected that interstitial hydrogen will migrate preferentially to areas of highest strain states. Under the conditions of rotary bend cyclic strain, it is likely that strain fields from hydrogen interact with the fatigue strains to reduce fatigue life.

In Regime 3, fatigue cycling occurs entirely in the elastic austenitic phase and there does not seem to be any differences in the fatigue behavior with hydrogen concentration.

The three fatigue regimes can also be analyzed with respect to the strain level and fatigue life, similar to the phenomenologically derived Coffin-Manson relationship:

$$N^\beta \Delta \epsilon_p = C$$

where  $C$  and  $\beta$  are constants, and  $\Delta \epsilon_p$  is the plastic strain per cycle [29]. Manson and others have shown  $b$  to be related to ductility and ranges between 0.5 to 0.75 for bcc and fcc materials with the second material constant,  $C$ , also related to ductility [30-31].

The stress-strain behavior of engineering materials changes with cyclic loading [29]. It has been shown that the Coffin-Manson equation is useful for analyzing elastic-plastic deformation. It follows that strain-based fatigue data is typically analyzed by superimposing the elastic and plastic  $\epsilon$ - $N$  curves [31]. Although this phenomenological relationship was originally derived for thermal [30] or mechanical cycling [31], it is interesting to follow Melton and Mercier [14] and apply the concept to fatigue behavior in NiTi.

The constant  $\beta$  was calculated for each hydrogen level in Regimes 1 and 2 and presented in Table II. By inspection of Figures 1 and 2, the highest strain values result in nearly constant fatigue life, irrespective of the hydrogen content. Consequently, the power law exponents in Regime 1 vary considerably for all H contents, suggesting that this is an inappropriate analysis approach. In contrast, the  $\beta$  constants for Regime 2 are much more similar and fall within the range -0.32 to -0.44. There does not appear to be a trend with hydrogen content within the limits studied in this investigation.

Table II: Coffin-Manson  $\beta$  Values for Regimes 1 and 2

Regime	H Content (wppm)	$\beta$ Value
1	10	-1.93
1	35	-1.48
1	50	0.26
1	80	-3.72
2	10	-0.41
2	35	-0.44
2	50	-0.32
2	80	-0.39

Previous zero-mean strain fatigue investigations of NiTi have exponents similar to those obtained in this investigation. For example, Melton and Mercier calculated a  $\beta$  value of approximately -0.23 for annealed NiTi with an  $M_s$  of 30°C and tested at 22°C. As such, this corresponds to non-transforming

martensitic fatigue behavior. [14] Thermomechanically processed martensite with 70°C  $A_f$  has a corresponding  $b$  of -0.44 between 1.45 and 4% strain in rotary bend testing [32]. This difference in power-law exponent in the two studies of martensite is likely due to difference in composition and processing conditions. Other researchers have also calculated  $\beta$  values for superelastic NiTi that closely match those calculated in Regime 2 for transforming NiTi. [18-19, 32]. For example, analysis of published data from superelastic NiTi ( $A_f = 10^\circ\text{C}$ , tested at 20°C) had a  $b$  exponent of -0.33 [17]. A recent study of low-cycle fatigue of superelastic stent-like devices show an exponent of approximately -0.42 with  $A_f = 30^\circ\text{C}$  tested at 37°C [19].

The use of a Coffin-Manson power-law analysis of NiTi fatigue behavior in the intermediate strain range appears to be useful for comparative purposes. However, it is inappropriate to assign mechanistic interpretation comparable to elastic-plastic fatigue behavior. Cyclic stress-induced transformations in NiTi differ from low-cycle fatigue in conventional engineering materials. As schematically illustrated in Figure 6, Regime 2 corresponds to the transition from elastic accommodation and incipient stress induced martensitic transformation. Since hydrogen does not influence the exponent values, this indicates that there is not a mechanistic change with these low-levels of hydrogen.

Finally, a more limited study was conducted to investigate the fatigue influence of 100-200 wppm hydrogen. As will be reported in another publication, there is significant decrease in fatigue life (one-two orders of magnitude) in Regimes 1 and 2. Furthermore, there is a decrease in the fatigue strain at  $10^7$  cycles compared to samples with 10-to 80-wppm hydrogen.

## Conclusions

This study investigated the effects of 10- to 80-wppm hydrogen on the fatigue behavior of superelastic NiTi. The following observations were made:

The data demonstrate a small but statistically significant trend of decreasing fatigue life with increasing hydrogen content. These effects were observed with as low as 50wppm at or above 1.4% strain under low-cycle ( $<10^4$ ), high strain ( $>1.4\%$ ) fatigue conditions. This strain-cycle regime corresponds to the strain regions for stress-induced martensite.

Increasing hydrogen concentration does not appear to affect fatigue life below 1.4% strain up to 80wppm H. This is especially noteworthy since many medical devices are designed for service in this regime.

Finally, there are no compelling data from the present investigation to indicate that stricter hydrogen limits should be considered for Nitinol devices.

## References

1. Proceedings of the Third International Conference on Shape Memory and Superelastic Technologies (SMST) 2000. S. Russell and A.R. Pelton editors. SMST International Committee. Pacific Grove, CA. (2001).
2. Pelton, B.L. *et al.* "Effects of Hydrogen in TiNi" Proceedings of the Second International Conference on Shape Memory and Superelastic Technologies (SMST) 1997. SMST International Committee. Pacific Grove, Ca. 1997. pg. 395.
3. Asaoko, T. *et al.* "Effect of Hydrogen on Mechanical and Shape Memory Properties of a Ti-Ni Alloy" Proceedings of the International Conference on Martensitic Transformations- ICOMAT 1992. (1993) pg. 1003-1008.
4. Yokoyama, K. *et al.* "Fracture Analysis of Hydrogen Charged Titanium Superelastic Alloy" Materials Transactions, Vol. 42, No. 1, January 2001. pg. 141.
5. Yokoyama, K. *et al.* "Degradation and Fracture of NiTi Superelastic Wire in an Oral Cavity" Biomaterials, Vol. 22, 2001. pg. 2257.
6. Yokoyama, K. *et al.* "Susceptibility to Delayed Fracture of Ni-Ti Superelastic Alloy" Materials Science and Engineering, Vol. A341, 2003. pg. 91.
7. Asaoka, K. "Hydrogen Embrittlement of Nickel-Titanium Alloy in Biological Environment" Metallurgical and Materials Transactions A, Vol. 33A, March 2002. pg. 495.
8. Pelton, A.R. *et al.* "Hydrogen Evolution From Nitinol" Proceedings of the Fourth International Conference on Shape Memory and Superelastic Technologies (SMST) 2003. Eds. A.R. Pelton, T. Duerig. Pacific Grove Ca: International Organization on SMST, 2004.
9. Pelton, A.R., *et al.*, "Structural and Diffusional Effects of Hydrogen in TiNi." Medical Device Materials- Proceedings of the Materials and Processes for Medical Devices Conference 2003. Ed. S. Shrivastava. ASM International, Materials Park, OH. (2004). Pg. 277.
10. Yamanaka, K. *et al.* "Hydride Formation of Intermetallic Compounds of Titanium-Iron, -Cobalt, -Nickel, and -Copper" Nippon Kagaku Daishi, 8, 1975. pg. 1267.
11. Burch, R. *et al.* "Absorption of Hydrogen by Titanium-Cobalt and Titanium-Nickel Intermetallic Alloy: Part 1- Experimental Results" J.C.S. Faraday I, 75, 1979, pg. 561.
12. Burch, R. *et al.* "Absorption of Hydrogen by Titanium-Cobalt and Titanium-Nickel Intermetallic Alloy: Part 2- Thermodynamic Parameters and Theoretical Models" J.C.S. Faraday I, 75, 1979, pg. 578.
13. Schmidt, R. *et al.* "Hydrogen Solubility and Diffusion in the Shape-Memory Alloy NiTi" J. Phys. Condens. Matter, Vol. 1, (1989) pg. 2473-2482.
14. K.N. Melton and O. Mercier: Acta Metall., 1979, Vol. 27, pg. 137-144.
15. Dauskardt, R.H. *et al.*: Shape Memory Materials, Proc. MRS Int. Meeting on Advanced Materials, K. Otsuka and K. Shimizu, eds., Materials Research Society, Pittsburgh, PA, 1989. Vol. 9. pg. 243-249.
16. Miyazaki, S., *et al.*, "Fatigue Life of Ti-50 at.% Ni and Ti-40Ni-10Cu (at.%) Shape Memory Alloy Wires." Mat Sci Eng A 1999; 273-275: 658-63.
17. M. Reinhold *et al.*, in SMST-2000: Proceedings of the International Conference on Shape Memory and Superelastic Technologies (SMST) 2000. Eds. S.M. Russell and A.R. Pelton. Pacific Grove, CA: International Organization on SMST, 2001, p. 397-403.
18. Tolomeo, D. *et al.*, "Cyclic Properties of Superelastic Nitinol: Design Implications." Proceedings of the International Conference on Shape Memory and Superelastic Technologies (SMST) 2000. Eds. S.M. Russell and A.R. Pelton. Pacific Grove, CA: International Organization on SMST, 2001, pg. 471.
19. Pelton, A.R., *et al.*, "Fatigue Testing of Diamond-Shaped Specimens." Proceedings of the International Conference on Shape Memory and Superelastic Technologies (SMST) 2003. Eds. A.R. Pelton, T. Duerig. Pacific Grove Ca: International Organization on SMST, 2004.
20. American Society For Testing and Materials. "ASTM F2063-00." Book of Standards Volume 13.01. 2003.
21. DiCello, J. in Proceedings of the International Conference on Shape Memory and Superelastic Technologies (SMST) 2003. Eds. A.R. Pelton, T. Duerig. Pacific Grove Ca: International Organization on SMST, 2004.
22. Beer, F., and Johnston, E.R., Mechanics of Materials. 2<sup>nd</sup> Edition. McGraw-Hill, New York. 1992. Pg. 189.
23. Nelson, H., in Hydrogen Effects in Materials- Proceedings of the Fifth International Conference on the Effect of Hydrogen on the Behavior of Materials 1994. Eds. A. Thompson, N. Moody. Mineral, Metals, and Materials Society (TMS), Warrendale, PA. (1996). Pg. 699.
24. Wu, S.K. and Wayman, C.M., Acta metall. 36 (1988), p. 1005.
25. Wu, S.K., Khachaturyan, A.G., and Wayman, C.M., Acta metall. 36 (1988), p. 2065.
26. Burch, R. and Mason, N.B., Z. Physikalisches Chemie Neue Folge 116 (1979), p. 185.
27. Wenzel, H., J. Less Common Metals 74 (1980), p. 351.
28. Wick, A., *et al.* "The Bending Behavior of NiTi" Journal De Physique IV. Colloque C8, Supplement au Journal de Physique III, Vol. 5, December 1995. pg. 789.
29. Suresh, S. Fatigue of Materials. 2<sup>nd</sup> Ed. Cambridge University Press. Cambridge, UK. 1998. pg. 256-259.
30. Manson, S. S. Thermal Stress and Low Cycle Fatigue. McGraw-Hill. New York, NY. 1966. pg. 125-192.
31. Coffin, L. F. and Tavernelli, J. F., Trans. A.I.M.E. 215, 794 (1959).
32. Wick, A., *et al.*, these Proceedings.
33. Pelton, A.R., *et al.*, SMST-2004

